Biochimica et Biophysica Acta 1838 (2014) 2994–3002

Contents lists available at ScienceDirect

Biochimica et Biophysica Acta

journal homepage: www.elsevier.com/locate/bbamem

Quantification of leakage from large unilamellar lipid vesicles by fluorescence correlation spectroscopy

Kasper Kristensen [a,c], Jonas R. Henriksen [b,c], Thomas L. Andresen [a,c,*]

[a] Department of Micro- and Nanotechnology, DTU Nanotech, Technical University of Denmark, DK-2800 Kongens Lyngby, Denmark
[b] Department of Chemistry, DTU Chemistry, Technical University of Denmark, DK-2800 Kongens Lyngby, Denmark
[c] Center for Nanomedicine and Theranostics, Technical University of Denmark, DK-2800 Kongens Lyngby, Denmark

ARTICLE INFO

Article history:
Received 6 April 2014
Received in revised form 2 July 2014
Accepted 7 August 2014
Available online 15 August 2014

Keywords:
Fluorescence correlation spectroscopy
Lipid vesicles
Leakage
Antimicrobial peptides
Peptide–lipid membrane interactions
Pore formation

ABSTRACT

Fluorescence correlation spectroscopy (FCS) is a powerful experimental technique that in recent years has found numerous applications for studying biological phenomena. In this article, we scrutinize one of these applications, namely, FCS as a technique for studying leakage of fluorescent molecules from large unilamellar lipid vesicles. Specifically, we derive the mathematical framework required for using FCS to quantify leakage of fluorescent molecules from large unilamellar lipid vesicles, and we describe the appropriate methodology for successful completion of FCS experiments. By use of this methodology, we show that FCS can be used to accurately quantify leakage of fluorescent molecules from large unilamellar lipid vesicles, including leakage of fluorescent molecules of different sizes. To demonstrate the applicability of FCS, we have investigated the antimicrobial peptide mastoparan X. We show that mastoparan X forms transient transmembrane pores in POPC/POPG (3:1) vesicles, resulting in size-dependent leakage of molecules from the vesicles. We conclude the paper by discussing some of the advantages and limitations of FCS as compared to other existing methods to measure leakage from large unilamellar lipid vesicles.

1. Introduction

Many membrane-active agents, such as antimicrobial peptides, can compromise the permeability barrier constituted by phospholipid membranes [1,2]. In order to study the membrane-destabilizing properties of these agents, synthetic large unilamellar lipid vesicles (LUVs) are often employed as model membrane systems. In typical experiments, LUVs are incubated together with a membrane-destabilizing agent that induces leakage of self-quenched fluorescent molecules from the LUVs. Leakage is then detected as an increase in fluorescence emission intensity due to fluorescence dequenching upon release of the fluorescent molecules from the LUVs [3,4]. Other approaches than the dequenching-based detection approaches have also been employed to detect leakage of fluorescent molecules from LUVs, for example, based on chromatographic separation of LUVs from released fluorescent molecules [5,6].

Another spectroscopic technique that has been used to study leakage of fluorescent molecules from LUVs is fluorescence correlation spectroscopy (FCS) [7–10]. In FCS, fluctuations in emission intensity from fluorescent particles diffusing across a small excitation volume are statistically analyzed via an autocorrelation function. The shape of this autocorrelation function depends, i.a., on the concentration and diffusion properties of the fluorescent particles [11,12]. Since fluorescent molecules encapsulated in LUVs are restricted to diffuse together with the LUVs, they will effectively have the same diffusion coefficient as the LUVs; see Fig. 1A. In contrast, free fluorescent molecules will have a higher diffusion coefficient than the LUVs; see Fig. 1B. Thereby, fluorescent molecules encapsulated in LUVs will make a different contribution to the autocorrelation function than the free fluorescent molecules, allowing us to use FCS to study the leakage process. In addition, by evaluating the diffusion properties of a fluorophore anchored to the membrane of the LUVs, FCS can also be used to evaluate the state of the LUVs during leakage; see Fig. 1C [13]. If leakage is due to formation of transmembrane pores, the LUVs will remain intact, and the diffusion coefficient of the lipid-anchored fluorophore will not change during the leakage process; see Fig. 1D. If leakage is due to membrane solubilization/micellization, the diffusion coefficient of the lipid-anchored fluorophore will increase as the fluorophore is incorporated into micelles. If vesicle aggregation and/or fusion occurs during leakage, the diffusion coefficient of the lipid-anchored fluorophore will decrease.

In this article, we evaluate the requirements for using FCS to quantify leakage of fluorescent molecules from LUVs. In particular, we derive the necessary mathematical framework and we present an appropriate experimental protocol that allows for FCS to be used to quantify leakage.

* Corresponding author at: Department of Micro- and Nanotechnology, DTU Nanotech, Technical University of Denmark, Produktionstorvet, Building 423, DK-2800 Kongens Lyngby, Denmark. Tel.: +45 45258168.
E-mail addresses: kakri@nanotech.dtu.dk (K. Kristensen), jhen@kemi.dtu.dk (J.R. Henriksen), tlan@nanotech.dtu.dk (T.L. Andresen).

http://dx.doi.org/10.1016/j.bbamem.2014.08.007
0005-2736/

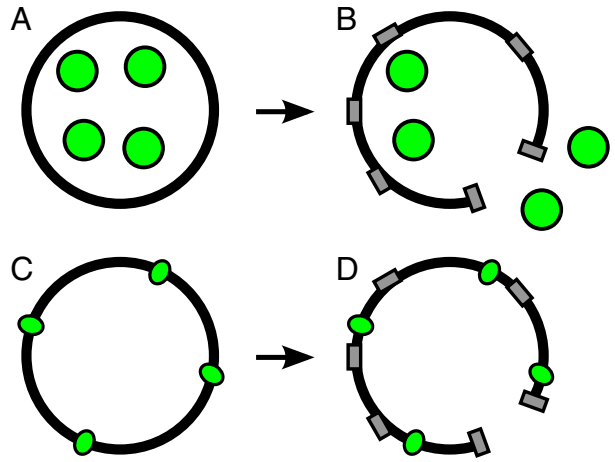

Fig. 1. Illustration of how the diffusion properties of fluorescent molecules are affected by leakage. (A) When fluorescent molecules are encapsulated in LUVs, they will be restricted to diffuse together with the LUVs. (B) Released fluorescent molecules will have a different diffusion coefficient than encapsulated fluorescent molecules. (C) When fluorophores are anchored to the membranes of the LUVs, they will diffuse together with the LUVs. (D) If leakage is due to formation of transmembrane pores, the diffusion coefficient of the lipid-anchored fluorophore will not change.

We also highlight some experimental pitfalls that are to be avoided if FCS is to be used to accurately quantify leakage.

To demonstrate the potential of FCS as a method to study leakage, we consider the natural antimicrobial peptide mastoparan X (MPX), isolated from the venom of the hornet *Vespa xanthoptera* [14]. MPX displays many archetypal features of antimicrobial peptides [15–18], including a short sequence of 14 amino acid residues, a strong net charge of +4, and an amphipathic α-helical membrane-bound structure [19,20]. It has previously been shown that MPX induces partial transient leakage of fluorescent molecules from LUVs, and that this leakage process is dependent on the size of the encapsulated molecules [21–25]. Here, we confirm these observations as we show that MPX-induced leakage from POPC/POPG (3:1) LUVs is due to the formation of transient transmembrane pores and that the size of these pores leads to size-selective leakage of fluorescent molecules ranging in size from ~500 Da to ~10 kDa.

We conclude the article by discussing some of the advantages and limitations of FCS as a method for studying leakage from LUVs.

2. Theory

We first consider the fundamental equations of FCS. For a single species of fluorescent molecules diffusing freely into and out of a three-dimensional Gaussian excitation volume, the autocorrelation function, $G(\tau)$, without triplet state contribution is given by [10,11]

$$G(\tau) = \frac{1}{N} g(\tau) = \frac{1}{N}\left(1+\frac{\tau}{\tau_D}\right)^{-1}\left(1+\frac{\tau}{S^2\tau_D}\right)^{-\frac{1}{2}} \quad (1)$$

where τ is the lag time, N is the average number of fluorescent molecules in the excitation volume, S is the ratio of the axial to radial dimensions of the excitation volume, and τ_D is the characteristic translational diffusion time of the fluorescent molecules. In case there are multiple diffusing species of fluorescent molecules, the autocorrelation function is a weighted sum of the autocorrelation functions of the individual species [10,11]:

$$G(\tau) = \frac{1}{F_t^2}\sum_{i=1}^{n} B_i^2 N_i g_i(\tau) = \sum_{i=1}^{n} A_i g_i(\tau) \quad (2)$$

where B_i is the brightness (photon count rate per fluorescent molecule) of the fluorescent molecules of the ith species, N_i is the mean number of fluorescent molecules of the ith species in the excitation volume, $g_i(\tau)$ is the diffusion autocorrelation function (defined in Eq. (1)) of the fluorescent molecules ith species, A_i is the amplitude of the term in the autocorrelation function corresponding to the diffusion of the fluorescent molecules of the ith species, and

$$F_t = \sum_{i=1}^{n} B_i N_i \quad (3)$$

is the total photon count rate.

Next, we consider a solution of LUVs to which a leakage-inducing agent has been added. In this solution, there are two distinct diffusing species: free fluorescent molecules (index f) and LUVs encapsulating fluorescent molecules (index v). According to Eq. (2), the autocorrelation function is then given by

$$G(\tau) = A_f g_f(\tau) + A_v g_v(\tau) \quad (4)$$

where

$$A_f = \frac{B_f^2 N_f}{F_t^2} \quad (5)$$

and

$$A_v = \frac{B_v^2 N_v}{F_t^2}. \quad (6)$$

The fraction, L, of fluorescent molecules that has leaked out of the LUVs upon addition of the leakage-inducing agent is given by

$$L = \frac{N_f}{N_{f100}} \quad (7)$$

where N_{f100} is the value of N_f evaluated for an equivalent solution of LUVs in which all LUVs have released all of their contents. By the use of Eq. (5), we can rewrite Eq. (7) to

$$L = \frac{A_f F_t^2}{A_{f100} F_{t100}^2}. \quad (8)$$

To further rewrite Eq. (8), we use that the total photon count rate of a solution of LUVs to which a leakage-inducing agent has been added can be split into two terms: a term stemming from fluorescent molecules that have leaked out of the LUVs after addition of leakage-inducing agent to the solution and a term stemming from fluorescent molecules that have remained encapsulated in the LUVs after addition of leakage-inducing agent to the solution. Since both of these terms are a function of leakage, L, we get the following expression for the total photon count rate, F_t:

$$F_t = B_f N_{f100} L + B_e N_{f100}(1-L). \quad (9)$$

where B_e is the brightness of encapsulated fluorescent molecules. (Note that B_e differs from B_v in that B_e is the photon count rate per encapsulated fluorescent molecule whereas B_v is the apparent photon count rate per LUV.) By inserting Eq. (9) into Eq. (8) and using that $L = 100\%$ for an LUV solution in which all LUVs have released all of their contents, a quadratic equation in L is obtained

$$A_f(1-k)^2 L^2 + (2A_f k(1-k) - A_{f100})L + A_f k^2 = 0 \quad (10)$$

where $k = B_e/B_f$ is the brightness ratio between encapsulated and free fluorescent molecules.

The details on how to experimentally determine the parameters in Eq. (10) to calculate leakage, L, are given in Section 3.3.2. However, before proceeding to this section, a few comments should be made regarding Eq. (10). Firstly, it should be noted that when setting $k = 1$ in Eq. (10), we obtain an expression that is completely analogous to previously derived expressions to determine the LUV-bound fractions of fluorescently-labeled proteins by FCS [26,27]. However, in the present study, this simplified expression will not be used as $k \neq 1$ in our experimental system.

Secondly, it should be noted that as F_t in our experimental setup is a direct output parameter of each individual FCS recording, N_f and N_{f100} could both be estimated directly from experimental autocorrelation curves by the use of Eqs. (4) and (5), provided that B_f is determined in a control experiment. Then leakage could be calculated directly using Eq. (7). This approach would certainly be simpler than solving the quadratic equation in Eq. (10). However, in our experience, this approach leads to larger uncertainties in the determined values of L than when solving Eq. (10). The reason for this is related to small experimental variations in F_t between individual experiments; since F_t is squared in Eq. (5), these small variations in F_t will lead to relatively larger variations in the determined values of L. In contrast, since the brightness ratio parameter, k, can be determined by averaging multiple experiments, Eq. (10) provides a more robust and accurate approach to calculate leakage; in other words, Eq. (10) is based on more precise estimates of the relative changes of F_t as a function of L than what is attainable by actually recording F_t in each individual experiment.

Finally, it should be mentioned that Eq. (10) is also applicable for calculating leakage of fluorescent molecules with a brightness distribution, such as fluorescently-labeled dextrans. This point is discussed in further detail in Section S1 in the Supporting material.

3. Materials and methods

3.1. Materials

1-Palmitoyl-2-oleoyl-*sn*-glycero-3-phosphocholine (POPC), 1-palmitoyl-2-oleoyl-*sn*-glycero-3-[phospho-rac-(1-glycerol)], sodium salt (POPG), and 1-palmitoyl-2-[11-(dipyrromethaneboron difluoride)undecanoyl]-*sn*-glycero-3-phosphocholine (TopFluor PC) were purchased from Avanti Polar Lipids (Alabaster, AL). N-(2-Hydroxyethyl)piperazine-N′-(2-ethanesulfonic acid) (HEPES) and the corresponding sodium salt (HEPES-Na), and NaCl were purchased from Sigma-Aldrich (St. Louis, MO). Rhodamine 6G chloride (Rh6G), Alexa Fluor 488 hydrazide, sodium salt (Alexa488), Alexa Fluor 488 dextran, 3000 MW (Alexa488-3kMW), and Alexa Fluor 488 dextran, 10,000 MW (Alexa488-10kMW) were purchased from Life Technologies (Carlsbad, CA). Mastoparan X (MPX) was purchased from GL Biochem (Shanghai, China) and further purified by semi-preparative HPLC (Waters semi-preparative HPLC equipped with a Waters 600 pump & controller and a Waters 2489 UV/vis detector, Waters, Milford, MA). The purity of the purified peptide was assessed to be >99% by analytical HPLC (Gilson analytical HPLC equipped with a Gilson 321 HPLC pump and a Gilson 155 UV/vis detector, Gilson, Middleton, MI). Furthermore, the peptide identity was confirmed by MALDI-TOF (Bruker Reflex IV MALDI-TOF spectrometer, Bruker, Billerica, MA).

3.2. Sample preparation

3.2.1. LUV preparation and characterization

POPC/POPG (3:1) solutions were prepared in chloroform/methanol (9:1). The organic solvent was removed under a gentle stream of nitrogen. The samples were subsequently kept in vacuum overnight to remove the residual solvent. The lipid films were hydrated in HEPES buffer (10 mM HEPES, 100 mM NaCl, pH 7.4) with vigorous vortexing every 5 min for a period of 30 min. The hydrated lipid suspensions were then subject to 5 freeze–thaw cycles by alternately placing the sample vials in an isopropanol/dry ice bath and a warm water bath. Next, the lipid suspensions were extruded 21 times through a 100 nm polycarbonate filter (Whatman, Maidstone, UK) using a mini-extruder (Avanti Polar Lipids) to form large unilamellar vesicles (LUVs). The size of the LUVs was checked by dynamic light scattering (ZetaPALS, Brookhaven Instruments, Holtsville, NY). Phosphorus concentrations of the LUV solutions were determined using the method of Rouser et al. [28], albeit with slightly modified reagent concentrations.

To prepare LUVs labeled with TopFluor PC, POPC/POPG (3:1) with 0.1 mol% TopFluor PC was dissolved in the initial chloroform/methanol (9:1) solution. The rest of the preparation protocol was then completely identical to the protocol used for preparation of unlabeled LUVs.

To prepare LUVs encapsulating fluorescent molecules, the HEPES buffer used to hydrate the POPC/POPG (3:1) lipid films was prepared with 4 or 30 μM Alexa488, 5 μM Alexa488-3kMW, or 2.5 μM Alexa488-10kMW. Concentrations of these fluorescent molecules were determined from absorbance values recorded by a NanoDrop 2000c spectrophotometer (NanoDrop Products, Wilmington, DE), utilizing (i) that the extinction coefficient of Alexa488 at maximum absorbance (usually at 495 nm) is 71,000 $cm^{-1}M^{-1}$ and (ii) that the degree of labeling of Alexa488-3kMW and Alexa488-10kMW was 1 and 2, respectively, as stated by the manufacturer. The rest of the preparation protocol was completely identical to the protocol for unlabeled LUVs, except that before the determination of phosphorous concentrations, LUV solutions were run on a size exclusion chromatography column (Sepharose CL-4B, GE Healthcare, Uppsala, Sweden) to remove the free fluorescent molecules from the LUV solutions.

3.2.2. MPX stock solutions

MPX stock solutions were prepared in HEPES buffer. To prevent loss of MPX due to adsorption to vial surfaces, MPX stock solutions were generally handled in Protein LoBind tubes (Eppendorf, Hamburg, Germany) and at high concentrations of at least 100 μM. To calculate the concentration of MPX stock solutions, the extinction coefficient of MPX at 220 nm was calculated to be 40,100 $cm^{-1}M^{-1}$ by correlating the MPX concentration determined by an Antek 8060 chemiluminescent nitrogen detector (PAC, Houston, TX) to the absorbance of the same MPX sample, determined by a NanoDrop 2000c spectrophotometer. Given this extinction coefficient, MPX concentrations of stock solutions were then always determined by recording the absorbance at 220 nm using the NanoDrop 2000c spectrophotometer.

3.3. FCS experiments

3.3.1. Experimental setup

FCS measurements were performed using a DCS-120 confocal scanning FLIM system (Becker & Hickl, Berlin, Germany) connected to a Zeiss Axio Observer Z1 inverted microscope equipped with a C-Apochromat 40x/1.2 W Corr UV–VIS-IR water immersion objective (Carl Zeiss, Jena, Germany). The excitation source for the system was a 473 nm picosecond diode laser (BDL-473-SMC, Becker & Hickl) operated at a pulse repetition rate of 50 MHz. The incident excitation power at the objective rear aperture was measured by a PM100D optical power meter (Thorlabs, Goteborg, Sweden). After passing through a 485 nm long-pass filter (HQ485LP, Becker & Hickl) and a confocal pinhole, the fluorescence emission was detected with a HPM-100-40 hybrid detector connected to a SPC-150 module (Becker & Hickl). Lifetime-gating was used to partially suppress background noise. SPCM software (Becker & Hickl) was used to calculate the experimental autocorrelation curves. The curves were subsequently exported to be fitted by MATLAB (The MathWorks, Natick, MA). All samples were measured in uncoated μ-slide 8 wells (ibidi, Martinsried, Germany) by positioning the laser focus ~50 μm above the top of the coverslip. The acquisition time for all experiments was 5 min. The effective excitation volume was determined to be 1.0 fL by calibration with Alexa488 [29]. From the same calibration experiments, the S-parameter was determined to be 8.6 by weighted least squares fitting

of the experimental autocorrelation curves to the single-component autocorrelation function (Eq. (1)) [30]. The *S*-parameter was always fixed to this value when fitting all other experimental autocorrelation curves. Except for the experiments determining the *S*-parameter, all autocorrelation curves in this article were analyzed using unweighted least squares fitting. Autocorrelation curves dominated by single bright events were discarded in the data analysis.

3.3.2. Protocol to treat the FCS data

To conduct a leakage experiment, a number of samples with constant concentrations of fluorescent molecule-containing LUVs but varying concentrations of leakage-inducing agent should be mixed to prepare a number of samples with leakage levels ranging between 0% and 100%. Next, FCS should be used to acquire experimental autocorrelation curves from each of these samples. Leakage of the fluorescent molecules can then be quantified by treating the autocorrelation curves with the following protocol.

1. Determine the LUV diffusion time, τ_{Dv}, by fitting the single-component autocorrelation function (Eq. (1)) to the autocorrelation curve recorded from the LUV solution with 0% leakage, i.e., from an LUV solution to which no leakage-inducing agent has been added.
2. Determine the diffusion time of free fluorescent molecules, τ_{Df}, by fitting the single-component autocorrelation function (Eq. (1)) to the autocorrelation curve recorded from the LUV solution with 100% leakage, i.e., from an LUV solution to which so much leakage-inducing agent has been added that all of the LUVs have released all of their contents. Complete leakage should be confirmed by comparing the determined value of τ_{Df} to diffusion times determined from solutions prepared with only free fluorescent molecules and no LUVs.
3. Determine the correction parameter z_0 (see below for discussion about the parameter) by fitting the autocorrelation curve acquired from the solution with 0% leakage used in Step 1 with the equation

$$G(\tau) = A_{v0}(z_0 g_f(\tau) + g_v(\tau)) \tag{11}$$

with τ_{Dv} and τ_{Df} kept fixed to the values determined in Steps 1 and 2, respectively. A_{v0} is a floating parameter of the fit but it is not used in the subsequent data analysis.

4. Determine A_f for each autocorrelation curve of the leakage experiment by fitting each curve with a modified two-component autocorrelation function:

$$G(\tau) = (A_f + z_0 A_v) g_f(\tau) + A_v g_v(\tau) \tag{12}$$

with τ_{Dv} and τ_{Df} kept fixed to the values determined in Steps 1 and 2, respectively, and z_0 kept fixed to the value determined in Step 3. A_v is a floating parameter of the fit but it is not used in the subsequent data analysis. The value of A_{f100} is determined from the autocorrelation curve acquired from the LUV solution with 100% leakage used in Step 2.

5. Determine the brightness ratio, *k*, using the equation

$$k = \frac{F_0}{F_{100}} \tag{13}$$

where F_0 and F_{100} are the photon count rates of the solutions with 0% and 100% leakage used in Steps 1 and 2, respectively. In general, *k* should be determined by averaging multiple experiments.

6. Solve Eq. (10) for *L* using each of the values of A_f determined in Step 4 together with the value of A_{f100} determined in Step 4 and the value of *k* determined in Step 5.

The experimental autocorrelation curves recorded from LUV solutions with 0% leakage were fitted well with a one-component autocorrelation function (Eq. (1)). When these curves were fitted with a two-component autocorrelation function (Eq. (4)) we did not observe a significant improvement in the quality of the fit; yet, a small but non-zero value of A_f was obtained from the fit in these situations due to what must be described as a typical data fitting artifact that ubiquitously occurs whenever a superfluous parameter is added to the data fitting model. The correction parameter z_0 was introduced in Steps 3 and 4 to correct for this small but non-zero value of A_f at 0% leakage. If z_0 was not included in the protocol, then $A_f \neq 0$ for solutions with 0% leakage and *L* would be slightly overestimated, especially at low values of *L*.

Along these lines, we have also found that similar data fitting artifacts might give rise to a small but non-zero value of A_v when fitting Eq. (4) to solutions with only free dye. This effect might slightly bias the values of A_f obtained at 100% leakage. However, because we have defined that A_{f100} is the value of A_f at 100% leakage, this effect will not lead to biases in the calculated values of *L*; therefore, we did not correct for this effect in the data fitting.

In our experimental setup, the typical value of τ_{Dv} was ~4700 μs, albeit variations between individual LUV batches were observed. The typical values of τ_{Df} were ~43 μs for Alexa488, ~100 μs for Alexa488-3kMW, and ~210 μs for Alexa488-10kMW. The typical values of z_0 were 0.033 for Alexa488, 0.028 for Alexa488-3kMW, and 0.025 for Alexa488-10kMW. Typical leakage experiments were conducted using an excitation power of 10.9 μW, corresponding to $k = 0.85$ for Alexa488, $k = 0.96$ for Alexa488-3kMW, and $k = 0.95$ for Alexa488-10kMW.

3.3.3. Accuracy of the FCS method

Series of samples with varying degrees of encapsulated/free fluorescent molecules and constant total concentration of fluorescent molecules were prepared in order to simulate a leakage experiment. Briefly, the samples were prepared by mixing varying volumes of (i) a stock solution with 1 mM POPC/POPG (3:1) LUV encapsulating 4 μM Alexa488, 5 μM Alexa488-3kMW, or 2.5 μM Alexa488-10kMW with (ii) a stock solution with free Alexa488, Alexa488-3kMW, or Alexa488-10kMW, respectively, with total molecular concentrations identical to those of the LUV stock solutions. The mixed samples were vigorously vortexed before being transferred to the μ-slide 8 wells for examination by FCS. Experiments were conducted with an excitation power of 10.9 μW. The experimentally acquired autocorrelation curves were treated by the data treatment protocol introduced in the previous section.

3.3.4. Experimental pitfalls

We considered three effects that might compromise the accuracy of leakage values determined by FCS. Firstly, we evaluated the effect of the number of fluorescent molecules encapsulated per LUV, $\widetilde{B}$. For this purpose, we prepared two series of samples to simulate leakage experiments for two different values of $\widetilde{B}$. These series of samples were prepared from stock solutions of (i) 1 mM POPC/POPG (3:1) LUV encapsulating 4 or 30 μM Alexa488 and (ii) free Alexa488 with total molecular concentrations identical to those of the LUV stock solutions. The mixed samples were vigorously vortexed before being transferred to the μ-slide 8 wells for examination by FCS. FCS experiments were performed with an excitation power of 10.9 μW. The data analysis was conducted using Steps 1–4 of the data treatment protocol to evaluate the effect of $\widetilde{B}$ on the fractional amplitude of the free fluorescent molecules, $y_f = A_f/(A_f + A_v)$.

Secondly, we evaluated the effect of the brightness ratio between encapsulated and free fluorescent molecules, *k*. For this purpose, we prepared a series of samples to simulate a leakage experiment for two different values of *k*. This series of samples was prepared from stock solutions of (i) 1 mM POPC/POPG (3:1) LUV encapsulating 4 μM Alexa488 and (ii) free Alexa488 with total molecular concentration identical to that of the LUV stock solution. The mixed samples were vigorously vortexed before being transferred to the μ-slide 8 wells for

examination by FCS. FCS experiments were performed at two different excitation powers of 10.9 and 43.2 μW, corresponding to $k = 0.85$ and 0.59, respectively. The data analysis was conducted using Steps 1–4 in the data treatment protocol to evaluate the effect of k on A_f.

Thirdly, we evaluated the interactions of Alexa488, Alexa488-3kMW, Alexa488-10kMW, and Rh6G with POPC/POPG (3:1) LUVs. For this purpose, we prepared samples with 40 nM of Alexa488, Alexa488-3kMW, Alexa488-10kMW, or Rh6G in (i) buffer, (ii) solutions with 1 mM unlabeled POPC/POPG LUV (3:1), or (iii) solutions with 1 mM unlabeled POPC/POPG (3:1) LUV and 50 μM MPX. All samples were mixed in Protein LoBind tubes and vigorously vortexed for a few seconds before being transfered to the μ-slide 8 wells for examination by FCS. Experiments were conducted with an excitation power of 10.9 μW. For the data analysis, the diffusion time of the free fluorescent molecules, τ_{Df}, was determined by fitting the single-component autocorrelation function (Eq. (1)) to the autocorrelation curves recorded from the samples of free fluorescent molecules in buffer. The LUV diffusion time, τ_{Dv}, was set to 4700 μs, a typical diffusion time for LUVs. The correction parameter, z_0, was set to 0.033 for Alexa488 and Rh6G, 0.028 for Alexa488-3kMW, and 0.025 for Alexa488-10kMW, typical values of z_0. The rest of the data analysis was then conducted using Step 4 in the data treatment protocol to determine the fractional amplitude of the unbound fluorescent molecules, $y_f = A_f/(A_f + A_v)$, for each sample.

3.3.5. Interaction of MPX with POPC/POPG (3:1) LUVs

To investigate the capability of MPX to induce leakage from POPC/POPG (3:1) LUVs, variable volumes of 100 μM MPX stock solutions were transferred to Protein LoBind tubes containing POPC/POPG (3:1) LUVs encapsulating 4 μM Alexa488, 5 μM Alexa488-3kMW, or 2.5 μM Alexa488-10kMW. After addition of MPX, the final LUV concentrations of these samples were always 1 mM. Immediately after addition of MPX, each sample was vigorously vortexed for a few seconds and subsequently incubated for 1 h at room temperature. After this incubation period, the samples were transferred to the μ-slide 8 wells for examination by FCS. Experiments were conducted with an excitation power of 10.9 μW. Leakage, L, was calculated using the data treatment protocol. The diffusion times of Alexa488, Alexa488-3kMW, and Alexa488-10kMW were used together with the Stokes–Einstein relationship to determine the hydrodynamic radii of Alexa488, Alexa488-3kMW, and Alexa488-10kMW to estimate the size of the transmembrane pores.

To evaluate the mechanism by which MPX induces leakage from POPC/POPG (3:1) LUVs, variable volumes of 100 μM MPX stock solutions were transferred to Protein LoBind tubes containing POPC/POPG (3:1) LUVs labeled with TopFluor PC. After addition of MPX, the final LUV concentrations of these samples were always 1 mM. Immediately after addition of MPX, each sample was vigorously vortexed for a few seconds and subsequently incubated for 1 h at room temperature. After this incubation period, the samples were transferred to the μ-slide 8 wells for examination by FCS. The excitation power of these FCS experiments was 2.6 μW. The recorded autocorrelation curves were fitted using the single-component autocorrelation function (Eq. (1)) to obtain information about the effect of MPX on the apparent number of LUVs in the excitation volume, N, and the LUV diffusion time, τ_D.

4. Results and discussion

4.1. Accuracy of the FCS method

Samples with varying degrees of encapsulated/free fluorescent molecules and constant total concentration of fluorescent molecules were prepared in order to simulate a leakage process from 1 mM POPC/POPG (3:1) LUV encapsulating 4 μM Alexa488, 5 μM Alexa488-3kMW, or 2.5 μM Alexa488-10kMW. Fig. S2 in the Supporting material shows some examples of autocorrelation curves recorded from these samples. Fig. 2 shows the experimentally determined leakage level of these samples, L vs the simulated leakage level, L_{sim}. The good agreement between

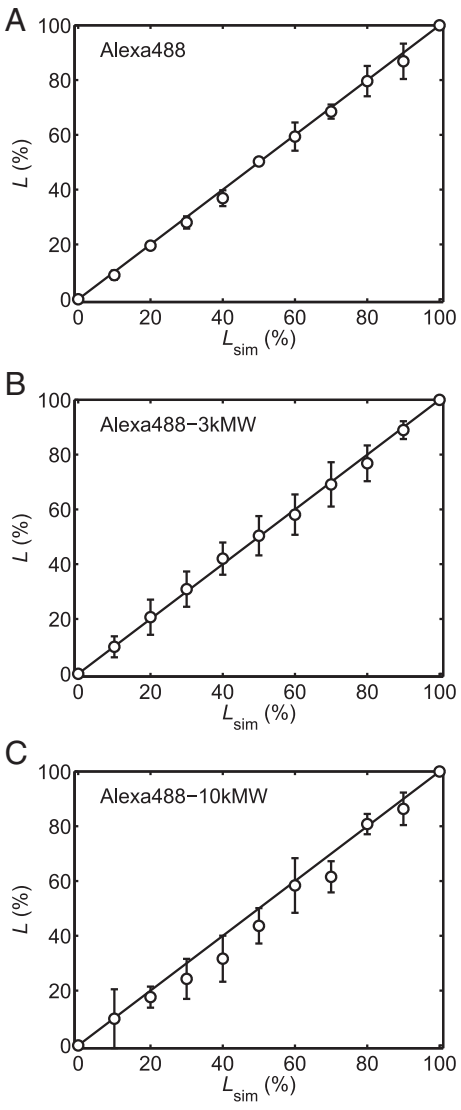

Fig. 2. Experimentally determined leakage value, L, vs simulated leakage value, L_{sim}, for series of samples simulating a leakage process from 1 mM POPC/POPG (3:1) LUV encapsulating 4 μM Alexa488 (A), 5 μM Alexa488-3kMW (B), or 2.5 μM Alexa488-10kMW (C). In all panels, the data are the average of three separate experiments. The error bars show the standard deviations. The error bars are not shown if they are smaller than the symbols. The L-values at $L_{sim} = 0\%$ and $L_{sim} = 100\%$ are, by definition, set to 0% and 100%, respectively. The data confirm that FCS can be used to accurately quantify leakage of fluorescent molecules of different sizes from LUVs.

L and L_{sim} confirms that FCS is applicable to accurately calculate leakage from LUVs of fluorescent molecules of different sizes.

4.2. Experimental pitfalls

In order to use FCS to obtain reliable estimates of leakage of fluorescent molecules from LUVs, a number of experimental pitfalls should be avoided. In the following sections, we highlight three of the most prominent examples of such pitfalls.

4.2.1. Number of fluorescent molecules encapsulated per LUV, $\widetilde{B}$

In a multicomponent autocorrelation function, written in a generalized form in Eq. (2), the amplitude pertaining to the ith species, A_i, scales with the square of the brightness of that species, B_i^2. Consequently, species with very high brightness will dominate such multicomponent autocorrelation functions. To illustrate the impact that this effect

might have on the accuracy of the calculated leakage values, we prepared two series of samples to simulate a leakage process from 1 mM POPC/POPG (3:1) LUV encapsulating 4 or 30 μM Alexa488. These two concentrations of encapsulated Alexa488 were from experiments found to correspond to the apparent number of Alexa488 molecules encapsulated per LUV, $\widetilde{B} = B_v/B_e$, being equal to 2.3 and 9.5, respectively. Fig. 3 shows the experimentally determined fractional amplitude of free Alexa488, $y_f = A_f/(A_f + A_v)$, as a function of the simulated leakage level, L_{sim}, for the two series of samples. The solid lines in the figure are plotted using Eq. S20 from the Supporting material. The data in Fig. 3 clearly demonstrate that the contribution of A_f to the entire amplitude of the autocorrelation curves decreases when brightness of the LUVs increases. This effect is especially pronounced for small values of leakage. However, if A_f only comprises a few percent of the entire amplitude of the autocorrelation function, then it will in many cases be difficult to obtain a reliable estimate of A_f, leading to poor resolution in the calculated leakage values. Along these lines, it can then be concluded that to use FCS to accurately calculate leakage, the number of fluorescent molecules encapsulated per LUV, $\widetilde{B}$, should be kept as low as possible. However, a lower limit to the number of fluorescent molecules encapsulated per LUV is dictated by the fact that a certain experimental photon count rate significantly above the background level is required. Accordingly, optimal experimental designs to accurately calculate leakage by FCS should balance the requirements for low numbers of fluorescent molecules per LUV and high photon count rates.

4.2.2. Brightness ratio between encapsulated and free fluorescent molecules, k

To meet the requirement for a low number of fluorescent molecules per LUV, a high photon count rate per fluorescent molecule is required. One way to increase the photon count rate per fluorescent molecule is to increase the intensity of the excitation source. However, we found that increasing the excitation intensity might significantly affect the ratio between the brightness of encapsulated and free fluorescent molecules, *k*. One possible hypothesis on the origin of this effect is that encapsulated fluorescent molecules are subject to a different local environment than free fluorescent molecules, causing the photophysical properties of encapsulated and free fluorescent molecules to be different. Another possible hypothesis is that the encapsulated fluorescent molecules are photobleached at a higher rate than the free fluorescent molecules; however, speaking against this latter hypothesis is the fact

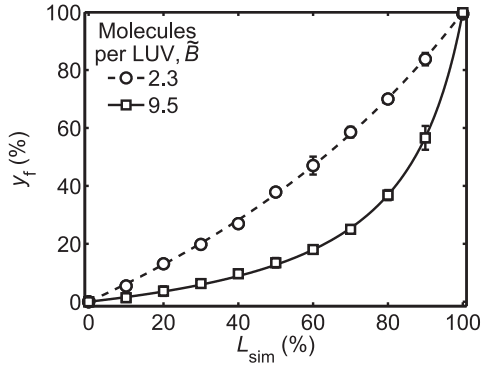

Fig. 3. Experimentally determined fractional amplitude of free Alexa488, $y_f = A_f/(A_f + A_v)$, vs simulated leakage level, L_{sim}, for two series of samples simulating a leakage process from 1 mM POPC/POPG (3:1) LUV encapsulating 4 or 30 μM Alexa488, corresponding to the apparent number of Alexa488 encapsulated per LUV, $\widetilde{B}$, being equal to 2.3 and 9.5, respectively. The data are the average of three separate experiments. The error bars show the standard deviations. The error bars are not shown if they are smaller than the symbols. The solid lines are calculated using Eq. S20 from the Supporting material. The results demonstrate that the concentration of fluorescent molecules inside the LUVs should be kept as low as possible for FCS to be used to accurately calculate leakage.

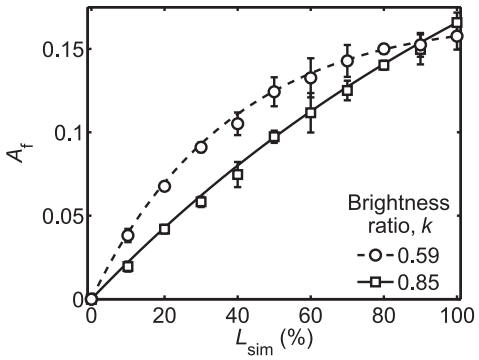

Fig. 4. Experimentally determined amplitude of the free Alexa488, A_f, vs simulated leakage level, L_{sim}, for a series of samples simulating a leakage process from 1 mM POPC/POPG (3:1) LUV encapsulating 4 μM Alexa488. FCS experiments were conducted for two different brightness ratios between encapsulated and free fluorescent molecules, $k = 0.85$ and 0.59, respectively. The data are the average of three separate experiments. The error bars show the standard deviations. The error bars are not shown if they are smaller than the symbols. The solid lines are calculated using Eq. S22 from the Supporting material. The data demonstrate that *k* should be kept close to 1 in order for Eq. 10 to be applicable for calculating leakage.

that the shape of the experimental autocorrelation curves does not significantly depend on the excitation intensity.

To evaluate the effect of *k* on the capability of FCS to accurately calculate leakage, we prepared a series of samples to simulate a leakage process from 1 mM POPC/POPG (3:1) LUV encapsulating 4 μM Alexa488. Two different excitation intensities, resulting in $k = 0.85$ and 0.59, respectively, were employed in the FCS experiments. Fig. 4 shows the experimentally determined amplitude of free Alexa488, A_f, as a function of the simulated leakage level, L_{sim}, as obtained using the two different excitation intensities. The solid lines in the figure are plotted using Eq. S22 from the Supporting material. For both excitation intensities, we observe that A_f is a monotonic function of L_{sim}, albeit for $k = 0.59$, we observe that A_f levels off at high values of L_{sim}. Thus, the data in Fig. 4 illustrate a problem arising when *k* is decreasing, namely, that the sensitivity of A_f to changes in leakage diminishes at high values of leakage. In addition, for even smaller values of *k* than those studied in Fig. 4, Eq. S22 from the Supporting material predicts a non-monotonic dependence of A_f to *L*, rendering Eq. (10) inapplicable to estimate leakage. We can thus conclude that the excitation intensity should be tuned to obtain *k*-values close to 1 in order for Eq. (10) to be applicable to accurately calculate leakage.

4.2.3. Interaction of fluorescent molecules with POPC/POPG (3:1) LUVs

Another important part of the experimental design is the choice of fluorescent molecules to be encapsulated inside the LUVs. In the present article, we used the hydrophilic anionic dye Alexa488, unconjugated or conjugated to dextran molecules. Another popular choice of dye for leakage studies by FCS is the cationic dye Rh6G. To investigate the suitability of each of these dyes for leakage experiments by FCS, we prepared series of samples in which 40 nM Alexa488, Alexa488-3kMW, Alexa488-10kMW, or Rh6G was mixed with (i) buffer, (ii) 1 mM unlabeled POPC/POPG (3:1) LUV, or (iii) 1 mM POPC/POPG (3:1) LUV and 50 μM MPX. Fig. 5 shows the fractional amplitude of the unbound fluorescent molecules, $y_f = A_f/(A_f + A_v)$, for the samples. For Alexa488, Alexa488-3kMW, and Alexa488-10kMW, y_f was always found to be close to 100%, indicating that none of these fluorescent molecules bind to the POPC/POPG (3:1) LUVs. In contrast, mixing Rh6G with 1 mM POPC/POPG (3:1) LUV yielded $y_f = 11\%$, indicating that a large fraction of the cationic Rh6G molecules bind to the surfaces of the anionic LUVs and thereby that Rh6G might be a poor choice of dye for leakage studies, at least under the experimental conditions used in this article. The risk of using Rh6G is further emphasized by the observation that when MPX is

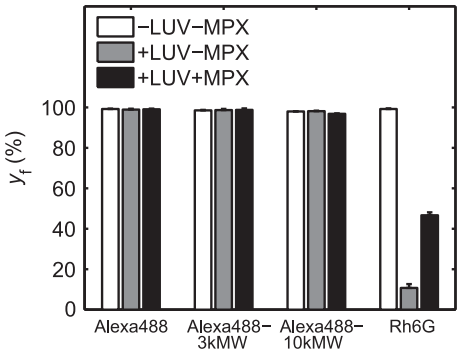

Fig. 5. Fractional amplitude of the unbound fluorescent molecules, $y_f = A_f/(A_f + A_v)$, for samples with 40 nM Alexa488, Alexa488-3kMW, Alexa488-10kMW, or Rh6G in (i) buffer, (ii) 1 mM unlabeled POPC/POPG (3:1) LUV, or (iii) 1 mM POPC/POPG (3:1) LUV and 50 μM MPX. The data are the average of three separate experiments. Error bars show the standard deviations. The data show that Alexa488, Alexa488-3kMW, and Alexa488-10kMW do not interact with the LUVs. In contrast, Rh6G clearly interacts with the LUVs. Upon addition of MPX, a significant fraction of the Rh6G molecules dissociates from the LUVs and/or the coverslips. This peptide-induced unbinding might easily be confused with peptide-induced leakage from LUVs.

present together with the LUVs, then y_f of Rh6G increase to 47%. Thus, the presence MPX entail an increasing contribution of unbound Rh6G to the autocorrelation function, probably because the polycationic MPX causes unbinding of Rh6G from the LUVs and/or the coverslips due to an entropy-driven counterion release effect. Such peptide-induced unbinding of Rh6G from the LUVs and coverslips might easily be mistaken for peptide-induced leakage from the LUVs. Thus, great caution should be taken when using Rh6G as the fluorescent marker in leakage experiments.

4.3. Interaction of MPX with POPC/POPG (3:1) LUVs

We used MPX to demonstrate the potential of our FCS-based protocol to study leakage. Fig. 6 shows MPX-induced leakage, *L*, vs the peptide-to-lipid ratio, [P]/[L] ratio, for samples in which variable concentrations of MPX had been incubated for 1 h with 1 mM POPC/POPG (3:1) LUV encapsulating 4 μM Alexa488, 5 μM Alexa488-3kMW, or 2.5 μM Alexa488-10kMW. From the figure, it is clear that MPX-induced leakage from POPC/POPG (3:1) LUVs is dependent on the size of the encapsulated fluorescent molecules; for example, Alexa488 was completely leaked out at [P]/[L] = 0.025, whereas only ~58% and ~23% of Alexa488-3kMW and Alexa488-10kMW, respectively, were leaked out at the same [P]/[L] ratio. However, at higher [P]/[L] ratios, Alexa488-3kMW and Alexa488-10kMW were also completely leaked out. Such size-dependent leakage has also previously been reported for MPX [24].

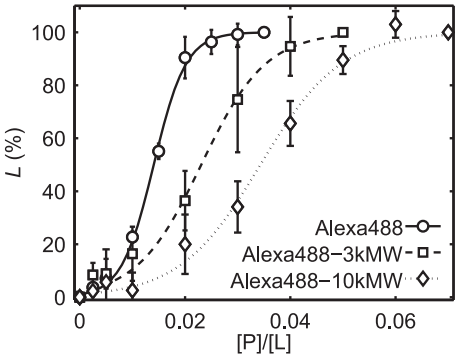

Fig. 6. MPX-induced leakage, *L*, from 1 mM POPC/POPG (3:1) LUV vs [P]/[L] ratio for samples in which MPX had been incubated for 1 h with the LUVs. The LUVs were encapsulating 4 μM Alexa488, 5 μM Alexa488-3kMW, or 2.5 μM Alexa488-10kMW. The data are the average of three separate experiments. The error bars show the standard deviations. The leakage values at the lowest and highest peptide-to-lipid ratios of a given experimental series correspond to 0% and 100% leakage, respectively, and, therefore they are, by definition, always set to 0% and 100%, respectively. Sigmoidal trendlines are added to guide the eye. Smaller fluorescent molecules were more effectively released than larger fluorescent molecules.

Fig. S3 in the Supporting material shows leakage at selected [P]/[L] ratios recorded after 10 min, 20 min, 1 h, and ~18 h incubation of MPX with POPC/POPG (3:1) LUVs. These data demonstrate that MPX-induced leakage of all three fluorescent molecules is a partial transient process, in which a rapid burst of leakage within the first few minutes is followed by a dramatic slowing down or complete cessation of leakage. Such biphasic leakage kinetics has previously been reported for MPX [21–25] as well as for many other antimicrobial peptides [31]. Due to this biphasic leakage kinetics, the leakage values recorded from samples incubated for 1 h are, by and large, representative of the leakage occurring within the first few minutes after addition of MPX to the LUVs.

To investigate whether MPX-induced leakage is due to formation of transmembrane pores or due to membrane solubilization, we incubated MPX together with 1 mM TopFluor PC-labeled POPC/POPG (3:1) LUV for 1 h. Fig. 7 shows the apparent mean number of LUVs in the excitation volume, *N*, and the LUV diffusion time, τ_D, vs the [P]/[L] ratio for these samples. From the figure, it is clear that both *N* and τ_D are largely independent of the [P]/[L] ratio. This observation strongly suggests that the LUVs remain intact during the leakage process; therefore, when held together with the data in Fig. S3, the data in Fig. 7 indicates that MPX-induced release of encapsulated molecules is due to the formation of transient transmembrane pores and not due to membrane solubilization.

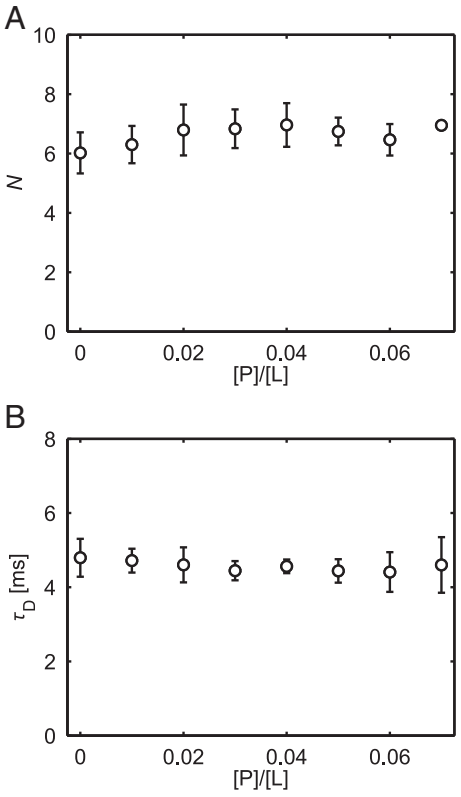

Fig. 7. Interaction of MPX with 1 mM TopFluor PC-labeled POPC/POPG (3:1) LUV. (A) The apparent mean number of LUVs in the excitation volume, *N*, vs [P]/[L] ratio. (B) The LUV diffusion time, τ_D, vs the [P]/[L] ratio. Data was recorded after 1 h incubation of MPX with the LUVs. The data are the average of three separate experiments. The error bars show the standard deviations. Error bars are not shown if they are smaller than the symbols. The fact that *N* and τ_D are largely independent on the [P]/[L] ratio indicate that leakage is due to the formation of transmembrane pores and not due to membrane solubilization.

This is in accordance with previously published data that shows that MPX only solubilizes POPC/POPG (3:1) LUVs at higher [P]/[L] ratios than what we consider in this article [32].

From the release profiles of Alexa488 and Alexa488-labeled dextrans in Fig. 6, we can get an estimate of the pore size. Thus, at low [P]/[L] ratios, Alexa488, with a hydrodynamic radius of ~0.6 nm, was more effectively released than were Alexa488-3kMW, with a hydrodynamic radius of ~1.3 nm, and Alexa488-10kMW, with a hydrodynamic radius of ~2.7 nm. This observation suggests that the typical pore radius at low [P]/[L] ratios is between ~0.6 nm and ~2.7 nm, in rough agreement with pore sizes previously suggested for MPX [24] as well as other antimicrobial peptides [5,6,33]. At higher [P]/[L] ratios, the Alexa488-labeled dextrans were completely released, suggesting that the pore radius at higher [P]/[L] ratio increases to above ~2.7 nm. However, the pore radii estimated from the hydrodynamic radii of the dextran molecules should be regarded with caution. Thus, dextran molecules are not perfect spheres with well-defined radii. Rather, dextran molecules are modeled as prolate ellipsoids with a short axis and a long axis, complicating attempts of relating their hydrodynamic radius to pore sizes [34]. In addition, it has been suggested that dextran molecules might pass through peptide-induced pores by reptation, further complicating the use of dextran molecules for sizing the pores [5]. Therefore, other types of fluorescently-labeled macromolecules might be more appropriate for accurately estimating the size of transmembrane pores. Nevertheless, in this article, we chose to use dextrans as that is also the common choice in most other articles in the literature. Under all circumstances, the data in Figs. 6 and 7 demonstrate that FCS can be used to obtain a high level of insight into the mechanisms underlying leakage induced by antimicrobial peptides as well as other leakage-inducing agents. The advantages and limitations of FCS as a method for studying leakage from LUVs are discussed in more detail in the following section.

4.4. Advantages and limitations of FCS as a method for studying leakage from LUVs

The central limitation of FCS as compared to the conventional quenching-based leakage assays is that FCS does not provide detailed information about the kinetics of the leakage process. In this article, we have used an experimental acquisition time of 5 min. This acquisition time could be shortened to approximately 1 min at the cost of slightly higher uncertainties in the calculated leakage values, but any leakage kinetics occurring on a time scale much faster than 1 min is beyond reach by FCS. However, in spite of this limitation, FCS still presents a number of interesting experimental advantages when compared to the conventional quenching-based leakage assays.

First, calculation of leakage by FCS is independent on the leakage mode of the fluorescent molecules. More specifically, calculation of leakage by FCS is independent on whether leakage proceeds by a graded process, in which all LUVs release part of their contents, or an all-or-none process, in which part of the LUVs release all of their contents and part of the LUVs release no contents. This is a great advantage of FCS as compared to the conventional quenching-based leakage assays in which the self-quenching factor of encapsulated fluorescent molecules is highly dependent on the nature of the leakage process [3,4].

Second, FCS requires only very low concentrations of fluorescent molecules inside the LUVs. Consequently, in a typical FCS leakage experiment, only a few fluorescent molecules are encapsulated in each LUV. Accordingly, when studying leakage by FCS, investigators are free to systematically vary the osmolarity and ionic strengths of the buffers inside and outside the LUVs. In contrast, the experimental designs in the conventional quenching-based leakage assays are restricted by the fact that fluorophore concentrations inside the LUVs have to be in the millimolar range to obtain quenching [3,4].

Third, as discussed in Section 4.3, FCS can be used to obtain rapid estimates of pore sizes in LUVs. Such estimates of pores sizes can, in principle, also be obtained by the conventional quenching-based leakage assays. However, as mentioned before, the quenching-based assays require that the concentration of fluorophores inside the LUVs be in the millimolar range; thus, if the fluorophores are conjugated to size marker molecule, such as dextran molecules, then the mass concentration of the size marker molecules inside the LUVs will be extremely high. In the FCS experiments, these crowded environments inside the LUVs will be avoided, minimizing risks that the kinetics of the leakage process will be affected by intermolecular interactions between the encapsulated size marker molecules. It should be mentioned that estimates of pore sizes in LUVs have also been obtained by chromatographic separation of LUVs from released fluorescent size marker molecules [5,6]. Although these chromatography-based methods require lower size marker concentrations than the conventional quenching-based leakage assays, they still require significantly higher concentrations than FCS.

Fourth, FCS reveals whether leakage is due to the formation of transmembrane pores or due to detergent-like solubilization of the lipid membrane [7,8]. In this article, we have evaluated the membrane integrity in a separate experiment on TopFluor PC-labeled LUVs. However, it should be mentioned that it would also be possible to measure leakage and membrane integrity in one single and fast two-color FCS experiment by considering leakage of a fluorescent marker that is spectrally separated from a membrane-anchored dye.

5. Conclusions

In this work, we considered FCS as a technique to study leakage of fluorescent molecules from large unilamellar lipid vesicles (LUVs). For this endeavor, we derived the necessary theoretical framework, and we highlighted the experimental pitfalls that might lead to inaccurate and/or false conclusions. To avoid these pitfalls, we showed that (i) the number of fluorescent molecules per LUV should be low, (ii) the brightness ratio between encapsulated and free molecules should be close to 1, and (iii) control experiments should ensure that the fluorescent molecules do not interact with the LUVs. FCS was then used to investigate leakage induced by the antimicrobial peptide mastoparan X (MPX). We showed that MPX induce size-dependent partial transient leakage from POPC/POPG (3:1) LUVs, and that leakage is due to the formation of transient transmembrane pores. In the final discussion, we concluded that FCS displays one central limitation when compared to the conventional quenching-based leakage assays, namely that the time resolution of the FCS experiments is poorer than the time resolution of the quenching-based assays. However, in the final discussion, we also concluded that FCS displays a number of advantages when compared to other existing methods to study leakage: (i) calculation of leakage by FCS is independent on whether the leakage process is an all-or-none process or a graded process, whereas calculation of leakage by the conventional quenching-based methods requires that the leakage mode is taken explicitly into account; (ii) FCS requires a much lower concentration of encapsulated fluorescent molecules per LUV than does other existing methods, allowing investigators to more freely vary the experimental conditions; (iii) FCS provides a fast method for sizing of transmembrane pores; and (iv) FCS reveals whether leakage is due to the formation of transmembrane pores or membrane solubilization.

Acknowledgements

We thank Lars Linderoth and Sofie Trier from Novo Nordisk for measuring MPX concentrations on the chemiluminescent nitrogen detector, and we thank Rasmus Irming Jølck, Lise Nørkjær Bjerg, and Rasmus Eliasen for help with the purification of MPX.

Financial support was kindly provided by the Technical University of Denmark (DTU) and the NanoMorph consortium funded by the Danish Council for Technology and Innovation.

Appendix A. Supplementary data

Supplementary data to this article can be found online at http://dx.doi.org/10.1016/j.bbamem.2014.08.007.

References

[1] M. Pasupuleti, A. Schmidtchen, M. Malmsten, Antimicrobial peptides: key components of the innate immune system, Crit. Rev. Biotechnol. 32 (2012) 143–171.
[2] W.C. Wimley, K. Hristova, Antimicrobial peptides: successes, challenges and unanswered questions, J. Membr. Biol. 239 (2011) 27–34.
[3] A.S. Ladokhin, W.C. Wimley, S.H. White, Leakage of membrane vesicle contents: determination of mechanism using fluorescence requenching, Biophys. J. 69 (1995) 1964–1971.
[4] K. Matsuzaki, O. Murase, K. Miyajima, Kinetics of pore formation by an antimicrobial peptide, magainin 2, in phospholipid bilayers, Biochemistry 34 (1995) 12553–12559.
[5] A.S. Ladokhin, M.E. Selsted, S.H. White, Sizing membrane pores in lipid vesicles by leakage of co-encapsulated markers: pore formation by melittin, Biophys. J. 72 (1997) 1762–1766.
[6] K. Matsuzaki, S. Yoneyama, K. Miyajima, Pore formation and translocation of melittin, Biophys. J. 73 (1997) 831–838.
[7] A. Pramanik, P. Thyberg, R. Rigler, Molecular interactions of peptides with phospholipid vesicle membranes as studied by fluorescence correlation spectroscopy, Chem. Phys. Lipids 104 (2000) 35–47.
[8] L. Yu, J.L. Ding, B. Ho, S.S. Feng, T. Wohland, Investigation of the mechanisms of antimicrobial peptides interacting with membranes by fluorescence correlation spectroscopy, Open Chem. Phys. J. 1 (2008) 62–79.
[9] L. Yu, L. Guo, J.L. Ding, B. Ho, S.S. Feng, J. Popplewell, M. Swann, T. Wohland, Interaction of an artificial antimicrobial peptide with lipid membranes, Biochim. Biophys. Acta 1788 (2009) 333–344.
[10] A. Blicher, K. Wodzinska, M. Fidorra, M. Winterhalter, T. Heimburg, The temperature dependence of lipid membrane permeability, its quantized nature, and the influence of anesthetics, Biophys. J. 96 (2009) 4581–4591.
[11] O. Krichevsky, G. Bonnet, Fluorescence correlation spectroscopy: the technique and its applications, Rep. Prog. Phys. 65 (2002) 251–297.
[12] J. Ries, P. Schwille, Fluorescence correlation spectroscopy, Bioessays 34 (2012) 361–368.
[13] M. Magzoub, K. Oglecka, A. Pramanik, L.E.G. Eriksson, A. Gräslund, Membrane perturbation effects of peptides derived from the N-termini of unprocessed prion proteins, Biochim. Biophys. Acta 1716 (2005) 126–136.
[14] Y. Hirai, M. Kuwada, T. Yasuhara, H. Yoshida, T. Nakajima, A new mast cell degranulating peptide homologous to mastoparan in the venom of Japanese hornet (*Vespa xanthoptera*), Chem. Pharm. Bull. (Tokyo) 27 (1979) 145–146.
[15] M. Zasloff, Antimicrobial peptides of multicellular organisms, Nature 415 (2002) 389–395.
[16] A.T.Y. Yeung, S.L. Gellatly, R.E.W. Hancock, Multifunctional cationic host defence peptides and their clinical applications, Cell. Mol. Life Sci. 68 (2011) 2161–2176.
[17] M.R. Yeaman, N.Y. Yount, Mechanisms of antimicrobial peptide action and resistance, Pharmacol. Rev. 55 (2003) 27–55.
[18] K.A. Brogden, Antimicrobial peptides: pore formers or metabolic inhibitors in bacteria? Nat. Rev. Microbiol. 3 (2005) 238–250.
[19] Y. Todokoro, I. Yumen, K. Fukushima, S.W. Kang, J.S. Park, T. Kohno, K. Wakamatsu, H. Akutsu, T. Fujiwara, Structure of tightly membrane-bound mastoparan-X, a G-protein-activating peptide, determined by solid-state NMR, Biophys. J. 91 (2006) 1368–1379.
[20] K. Wakamatsu, A. Okada, T. Miyazawa, M. Ohya, T. Higashijima, Membrane-bound conformation of mastoparan-X, a G-protein-activating peptide, Biochemistry 31 (1992) 5654–5660.
[21] G. Schwarz, A. Arbuzova, Pore kinetics reflected in the dequenching of a lipid vesicle entrapped fluorescent dye, Biochim. Biophys. Acta 1239 (1995) 51–57.
[22] A. Arbuzova, G. Schwarz, Pore kinetics of mastoparan peptides in large unilamellar lipid vesicles, Prog. Colloid. Polym. Sci. 100 (1996) 345–350.
[23] A. Arbuzova, G. Schwarz, Pore-forming action of mastoparan peptides on liposomes: a quantitative analysis, Biochim. Biophys. Acta 1420 (1999) 139–152.
[24] K. Matsuzaki, S. Yoneyama, O. Murase, K. Miyajima, Transbilayer transport of ions and lipids coupled with mastoparan X translocation, Biochemistry 35 (1996) 8450–8456.
[25] L.E. Yandek, A. Pokorny, P.F.F. Almeida, Wasp mastoparans follow the same mechanism as the cell-penetrating peptide transportan 10, Biochemistry 48 (2009) 7342–7351.
[26] Y.O. Posokhov, M.V. Rodnin, L. Lu, A.S. Ladokhin, Membrane insertion pathway of annexin B12: thermodynamic and kinetic characterization by fluorescence correlation spectroscopy and fluorescence quenching, Biochemistry 47 (2008) 5078–5087.
[27] L. Rusu, A. Gambhir, S. McLaughlin, J. Rädler, Fluorescence correlation spectroscopy studies of peptide and protein binding to phospholipid vesicles, Biophys. J. 87 (2004) 1044–1053.
[28] G. Rouser, A.N. Siakotos, S. Fleischer, Quantitative analysis of phospholipids by thin-layer chromatography and phosphorus analysis of spots, Lipids 1 (1966) 85–86.
[29] S. Rüttinger, V. Buschmann, B. Krämer, R. Erdmann, R. Macdonald, F. Koberling, Comparison and accuracy of methods to determine the confocal volume for quantitative fluorescence correlation spectroscopy, J. Microsc. 232 (2008) 343–352.
[30] T. Wohland, R. Rigler, H. Vogel, The standard deviation in fluorescence correlation spectroscopy, Biophys. J. 80 (2001) 2987–2999.
[31] W.C. Wimley, Describing the mechanism of antimicrobial peptide action with the interfacial activity model, ACS Chem. Biol. 5 (2010) 905–917.
[32] J.R. Henriksen, T.L. Andresen, Thermodynamic profiling of peptide membrane interactions by isothermal titration calorimetry: a search for pores and micelles, Biophys. J. 101 (2011) 100–109.
[33] S.J. Ludtke, K. He, W.T. Heller, T.A. Harroun, L. Yang, H.W. Huang, Membrane pores induced by magainin, Biochemistry 35 (1996) 13723–13728.
[34] M.P. Bohrer, W.M. Deen, C.R. Robertson, J.L. Troy, B.M. Brenner, Influence of molecular configuration on the passage of macromolecules across glomerular capillary wall, J. Gen. Physiol. 74 (1979) 583–593.